Relative Ground and Excited-State pK_a Values of Phytochromobilin in the Photoactivation of Phytochrome: A Computational Study

O. Anders Borg[†] and Bo Durbeej*[,‡]

Department of Chemistry, University of Siena, Via Aldo Moro 2, I-53100 Siena, Italy, and Department of Quantum Chemistry, Uppsala University, Box 518, S-75120 Uppsala, Sweden

Received: April 10, 2007; In Final Form: July 17, 2007

The conversion of the plant photoreceptor phytochrome from an inactive (Pr) to an active form (Pfr) is accomplished by a red-light induced $Z \rightarrow E$ photoisomerization of its phytochromobilin chromophore. In recent years, the question whether the photoactivation involves a change in chromophore protonation state has been the subject of many experimental studies. Here, we have used quantum chemical methods to calculate relative ground and excited-state pK_a values of the different pyrrole moieties of phytochromobilin in a protein-like environment. Assuming (based on experimental data) a Pr *ZaZsZa* chromophore and considering isomerizations at C15 and C5, it is found that moieties B and C are the strongest acids both in the ground state and in the bright first singlet excited state, which is rationalized in simple geometric and electronic terms. It is also shown that neither light absorption nor isomerization increases the acidity of phytochromobilin relative to the reference Pr state with all pyrrolenic nitrogens protonated. Hence, provided that the subset of chromophore geometries under investigation is biologically relevant, there appears to be no intrinsic driving force for a proton-transfer event. In a series of benchmark calculations, the performance of ab initio and time-dependent density functional theory methods for excited-state studies of phytochromobilin is evaluated in light of available experimental data.

Introduction

Phytochromes are plant photoreceptors that control processes like germination and flowering in response to environmental light conditions.[1−4] First found and characterized in higher plants, these biliproteins have recently been discovered also in cyanobacteria and even nonphotosynthetic bacteria and fungi.[5] The biological function of phytochrome is governed by the conformational switching between inactive red-light absorbing (Pr, $\lambda_{max,abs} \sim 660$ nm) and active far-red-light absorbing (Pfr, $\lambda_{max,abs} \sim 730$ nm) forms.[6] Pr and Pfr are reversibly photointerconvertible, and their ratio determines the signaling state of the protein. Red-light illumination shifts the equilibrium toward Pfr and activates signal transduction pathways underlying the physiological response, whereas far-red light restores Pr and cancels the response.[6] The chromophore of plant phytochrome, phytochromobilin (PΦB), is a methine-bridged tetrapyrrole (bilin) that is covalently attached to the apoprotein through a thioether linkage between the C3 vinyl group on ring A and a cysteine residue (Figure 1).[7]

Characterizing Pr and Pfr structurally has been a difficult objective, despite long-standing efforts.[3,4] As for the chromophore, it is likely that it adopts an extended, rather than cyclic, conformation. Furthermore, ^{1}H NMR spectra of phytochrome chromopeptide fragments[8] and resonance Raman (RR) vibrational spectroscopy studies[9−13] indicate that PΦB adopts a C15-*Z* configuration in Pr and a C15-*E* configuration in Pfr. Accordingly, it is generally believed, although not yet unambiguously established, that the photoactivation involves a C15 $Z \rightarrow E$ photoisomerization of PΦB.

As to the overall structure of PΦB, experimental studies are without a consensus view. RR spectra indicative of C4-*Z* C5-*anti* C10-*E,anti* C15-*Z,syn* (*ZaEaZs*) and C4-*Z* C5-*anti* C10-*E,anti* C15-*E,anti* (*ZaEaEa*) configurations in Pr and Pfr, respectively, have been recorded.[10,12] This suggests that the photoactivation proceeds by way of isomerization (C15 *Z,syn* → *E,anti*) about both bonds of the CD methine bridge. Other RR spectra have led to proposals of a *ZaZsZa* configuration in Pr,[11,13] which has also been put forward in a theoretical study correlating calculated absorption maxima of different PΦB structures with experimental data.[14] Although no X-ray crystallographic structures of plant phytochrome are available, the structure of the chromophore-binding domain of a Pr bacteriophytochrome was recently determined,[15] followed by an overall low-resolution solution-state structure from small-angle X-ray scattering.[16] The chromophore of bacteriophytochrome, biliverdin IXα (BV), is an oxidized precursor to PΦB in higher plants and has a double bond between C2 and C3. Consistent with the RR data on plant phytochrome reported by Hildebrandt and co-workers[11,13] regarding the configuration about C10 and C15 but different with respect to C5, the X-ray structure supports a *ZsZsZa* (rather than *ZaZsZa*) geometry in Pr.[15] It was also found that the thioether linkage attaching BV to the apoprotein involves a different cysteine residue and C3 side-chain carbon atom ($C3^2$ instead of $C3^1$) than invariably employed by plant phytochrome, which may be the origin of the different C5 configuration in bacteriophytochrome.

Although pertaining to the Pr form only, the bacteriophytochrome X-ray structure[15] also provides information of relevance for establishing a chromophore isomerization pathway, with possible implications for all phytochrome classes. In particular, Lagarias and co-workers[3,4] have argued that thermal single-bond rotations at C5 or C10 are unlikely to accompany a C15

* Corresponding author. E-mail: bo.durbeej@kvac.uu.se.
† Uppsala University.
‡ University of Siena.

10.1021/jp0727953 CCC: $37.00
Published on Web 09/11/2007

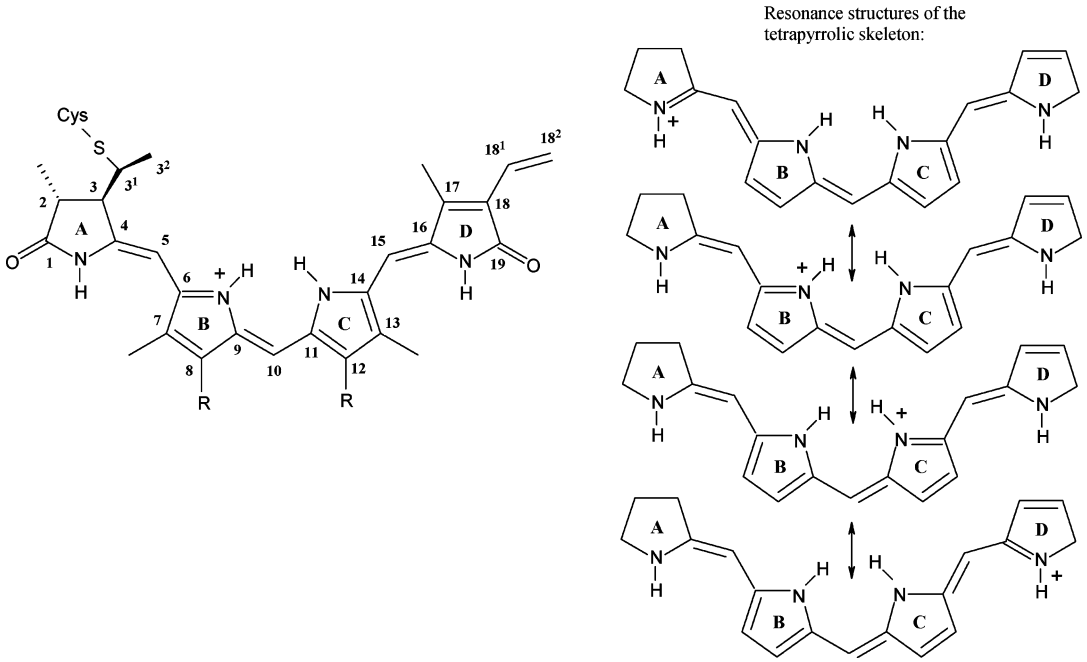

Figure 1. Chemical structure of C4-*Z* C5-*anti* C10-*Z,syn* C15-*Z-anti* phytochromobilin in its parent protonated form. R = CH_2CH_2COOH.

$Z \rightarrow E$ photoisomerization, because rings A, B, and C are much more tightly packed by protein residues than D.[15] Furthermore, the C15 single-bond rotation implicated by RR experiments[10,12] appear to be sterically disfavored.[3,4,15] Taken together, these observations would suggest that the photoactivation is governed solely by a C15 $Z \rightarrow E$ double-bond photoisomerization.[3,4] Support for this notion has been obtained from UV-vis spectral measurements on synthetic, configurationally restricted, BV derivatives assembled with bacteriophytochrome.[17]

On the other hand, it has also been reported that a thermal single-bond rotation at C5 may follow the formation of the photoisomerized Lumi-R photoproduct (the first intermediate of the Pr → Pfr reaction cycle).[13,18,19] Presenting RR data in favor of *ZaZsZa* and *ZaZsEa* configurations in Pr and Lumi-R, Mroginski et al. also proposed that the subsequent relaxation steps of the reaction cycle could involve at least a partial C5 *anti* → *syn* isomerization.[13] Studying cyanobacterial phytochrome, which utilizes a chromophore (phycocyanobilin) differing from PΦB by carrying an ethyl rather than vinyl group at C18, van Thor et al. reported ^{13}C NMR experiments predicting a *ZsZsZa* configuration in Pr and pointing to the possibility that the $Z \rightarrow E$ photoisomerization actually occurs at C4 (rather than C15), and is followed by a thermal *syn* → *anti* isomerization at C5.[18] A C5 *syn* → *anti* rotation of phycocyanobilin has also been discussed in light of results from mid-infrared spectroscopy experiments.[19]

The protonation state of the pyrrolenic nitrogens of PΦB is another issue of substantial interest in phytochrome research. Upon formation of the signaling Pfr form, a change in protonation state is conceivable because proton-transfer reactions are of fundamental importance for the function of related photoreceptors such as the rhodopsins.[20−22] Based on RR[11,23−25] and Fourier transform infrared (FTIR)[26,27] studies of plant phytochrome, there is agreement on all four nitrogens being protonated in Pr (protonated PΦB, Figure 1). Although the FTIR data furthermore indicate that the nitrogens are protonated also in Pfr (as well as in all intermediate states connecting Pr and Pfr),[26,27] the RR spectra of Pfr are conflicting. Inferring the transfer of one proton to the surrounding protein, those by Mizutani et al. argue for a *neutral* chromophore in this state,[23,24] whereas those by Schaffner and co-workers are compatible with a protonated species.[11,25] Rather than a net loss of one proton, studies have also been reported pointing to a proton release and uptake mechanism involving a neutral chromophore in an intermediate state.[28,29] Finally, as for NMR studies, both solution and solid-state ^{15}N NMR data on cyanobacterial phytochrome favor a protonated chromophore in both Pr and Pfr.[30,31]

Recently, the possibility that the chromophore protonation state changes during the photoactivation was assessed in an indirect fashion through the computation of ground and excited-state potential-energy surfaces of PΦB.[32−34] Thereby, it was found that neutral forms of the chromophore are much less likely to photoisomerize than the protonated form, in support of the notion that all pyrrolenic nitrogens remain protonated. Using a more direct approach, the aim of the present work is to investigate whether there is a significant difference in the *intrinsic* acidity of PΦB with respect to configuration that facilitates proton transfer to the surrounding protein as the chromophore isomerizes. To this end, relative pK_a values of protonated *ZaZsZa*, *ZaZsEa*, *ZaZsZs*, and *ZaZsEs* PΦB are calculated using quantum chemical methods. This particular set of configurations allows for an assessment of changes in acidity due to C15 $Z \rightarrow E$ isomerization as well as to an additional C15 single-bond rotation event, and accounts for a number of different chromophore isomerization pathways.[3,4,10,12,15,17] From computations on a set of other configurations, the effect of a thermal single-bond rotation at C5[13,18,19] is investigated as well. By calculating pK_a's of all pyrrole moieties in both the ground (S_0) and the bright first singlet excited (S_1) $\pi\pi^*$ state responsible for the photochemistry, we will estimate the relative acidities of the rings and the two states and take into consideration both thermal and excited-state proton-transfer reactions. Since several excited-state quantum chemical methods are employed, this work furthermore serves as a useful benchmark for future computational studies of bilin chromophores.

Methods

Computational Details. All calculations were carried out using a computational model with the full conjugated π-system

of PΦB retained and the thioether linkage, the carboxyl side chains of rings B and C, and the methyl group of each ring replaced by hydrogen atoms. Ground and excited-state geometries of protonated ($P\Phi B^+$) and neutral ($n_XP\Phi B$, where X = {A, B, C, D} specifies the deprotonated ring) forms of the chromophore were optimized using the B3LYP hybrid density functional method and the ab initio CIS (configuration interaction singles) method, respectively, in combination with the 6-31G(d,p) basis set. Enthalpy and free-energy corrections at $T = 298.15$ K were obtained by subsequently performing B3LYP/6-31G(d,p) and CIS/6-31G(d,p) frequency calculations. All structures were thereby identified as potential-energy minima.

The pK_a calculations were preceded by a benchmark investigation aimed at first identifying a method allowing for accurate and affordable studies of PΦB photochemistry. Accordingly, vertical $S_1 \leftarrow S_0$ excitation energies at optimized ground-state geometries and vertical $S_1 \rightarrow S_0$ emission energies at optimized excited-state geometries were calculated using both ab initio and density functional theory (DFT) methods. Three ab initio methods (CIS, CIS(D),[35] and SAC-CI[36,37]) and two hybrid functionals (B3LYP and PBE0[38] within a time-dependent (TD) formalism[39−42]) were considered. The basis set used for these calculations was 6-31G(d,p) (6-31G for the much more expensive SAC-CI method).

CIS(D) is an extension of the CIS method and includes the effect of double excitations by means of perturbation theory. SAC-CI (symmetry-adapted cluster configuration interaction) is a high-level method that explicitly accounts for both single and double excitations, and that uses a reference state corresponding to an exponential cluster expansion rather than a Hartree−Fock (HF) ground-state wave function (as employed by CIS and CIS(D)). The SAC-CI calculations were carried out with thresholds for selection of ground and excited-state double-excitation operators set to either 1×10^{-5} and 1×10^{-6} au (level-1) or 5×10^{-6} and 5×10^{-7} au (level-2), respectively. Excitations from core orbitals were excluded in all ab initio calculations.

The performance of the different methods was then assessed by comparing calculated excitation and emission energies with experimental absorption and fluorescence data. On the basis of this comparison, the solvation free energies required for the computation of excited-state pK_a's were obtained by subjecting the optimized excited-state geometries to TD-B3LYP single-point calculations within the integral equation framework of the polarizable continuum model (IEF-PCM).[43,44] The choice of basis set (6-311G(2df,p)) and dielectric constant ($\epsilon = 4.0$) was established by extending the benchmark investigation to include also vertical TD-B3LYP excitation and emission energies from (i) gas-phase calculations with the 6-31++G(d,p), 6-311G-(2df,p) and 6-311++G(2df,p) basis sets and (ii) IEF-PCM calculations with the 6-311G(2df,p) basis set and the dielectric constant chosen to represent either a protein environment ($\epsilon = 4.0$) or an aqueous solution ($\epsilon = 78.39$). The solvation free energies required for the computation of ground-state pK_a's, in turn, were obtained by performing B3LYP-IEF-PCM single-point calculations on optimized ground-state geometries, using the same basis set and value for the dielectric constant as employed in the excited-state pK_a calculations.

The observation (see below) that TD-B3LYP-IEF-PCM emission energies agree with experimental fluorescence data to within ∼0.2 eV indicates that single-reference CIS theory provides accurate excited-state geometries. To further explore this important issue, excited-state geometries were for a few systems also optimized using three other methods for which analytic gradients are available: the multi-reference CASSCF (complete active space self-consistent field) method,[45,46] the TD-DFT method of Furche and Ahlrichs[47] and SAC-CI. These optimizations were carried out with the cc-pVDZ[48] (CASSCF), the Karlsruhe SVP[49] (TD-DFT), and the smaller 6-31G (SAC-CI) basis set, respectively. The CASSCF method accounts for nondynamic electron correlation effects on excited-state geometries, and TD-B3LYP and SAC-CI account for dynamic electron correlation. Since the dominant contributions to the π-orbitals primarily responsible for the photochemistry are from the carbons of the CD methine bridge,[32] the CASSCF calculations employed an active space consisting of four electrons distributed in four orbitals (CASSCF(4,4)). The TD-DFT calculations were performed using B3LYP, and the SAC-CI calculations using "level-1" thresholds.

All calculations were carried out with the GAUSSIAN 03,[50] MOLCAS 6.2[51,52] (for CASSCF), or TURBOMOLE[53] (for TD-DFT geometry optimizations) suites of programs.

pK_a Calculations. The pK_a of a species HA in a medium m is related to the standard Gibbs free-energy change of the reaction

$$HA \rightarrow A^- + H^+ \quad (1)$$

in the medium, according to

$$pK_a = [G_m(A^-) + G_m(H^+) - G_m(HA)]/RT \ln 10 \quad (2)$$

Using a dielectric continuum model to implicitly represent the solvent medium, it is conceptually straightforward to calculate pK_a values quantum chemically by treating gas-phase and solvation contributions separately. The free energies $G_m(A^-)$ and $G_m(HA)$ can then be estimated by adding the solvation contributions $\Delta G_{solv,m}(A^-)$ and $\Delta G_{solv,m}(HA)$ readily computed within the framework of such a model to the gas-phase free energies $G_{gas}(A^-)$ and $G_{gas}(HA)$ obtained from standard frequency calculations. Furthermore, experimental values can be used for $G_{gas}(H^+)$ and $\Delta G_{solv,m}(H^+)$.

Although using this procedure to calculate quantitatively accurate pK_a's is a challenging task demanding both reliable gas-phase computations and an adequate description of the solvent,[54−59] many different combinations of DFT method and continuum solvation model have been shown to reproduce experimental pK_a's of a variety of organic compounds in different solvents,[60−64] DNA nucleobases,[65,66] and amino acid residues in protein environments.[67−69] In the present work, the aim is to compute relative pK_a values with respect to pyrrole moiety and PΦB configuration. Thus, errors due to methodological deficiencies are largely expected to cancel. The difference between the pK_a's of ring X in chromophore configuration *Y*, and ring A in configuration *ZaZsZa* (throughout used as reference), was computed as

$$\Delta pK_a^I = [G_{gas}^I(Y\ n_X P\Phi B) + \Delta G_{solv,m}^I(Y\ n_X P\Phi B) - G_{gas}^I(Y\ P\Phi B^+) - \Delta G_{solv,m}^I(Y\ P\Phi B^+) - G_{gas}^I(ZaZsZa\ n_A P\Phi B) - \Delta G_{solv,m}^I(ZaZsZa\ n_A P\Phi B) + G_{gas}^I(ZaZsZa\ P\Phi B^+) + \Delta G_{solv,m}^I(ZaZsZa\ P\Phi B^+)]/RT \ln 10 \quad (3)$$

where $I = \{S_0, S_1\}$ is the electronic state and the corresponding terms on the right-hand side were evaluated at geometries optimized for the state in question.

To calculate relative excited-state pK_a's ($\Delta pK_a^{S_1}$), the excited-state solvation free energy ($\Delta G_{solv,m}^{S_1}$) was approximated by the sum of the B3LYP-IEF-PCM ground-state solvation free

TABLE 1: Vertical Excitation ($S_1 \leftarrow S_0$) and Emission ($S_1 \rightarrow S_0$) Energies (in eV) of Protonated (PΦB$^+$) and Neutral (n_XPΦB) Forms of Phytochromobilin Calculated by Different Methods[a]

	CIS		CIS(D)		TD-B3LYP		TD-PBE0		SAC-CI/6-31G		
form	$S_1 \leftarrow S_0$	$S_1 \rightarrow S_0$	$S_1 \leftarrow S_0$	$S_1 \rightarrow S_0$	$S_1 \leftarrow S_0$	$S_1 \rightarrow S_0$	$S_1 \leftarrow S_0$	$S_1 \rightarrow S_0$	level-1 $S_1 \leftarrow S_0$	level-2 $S_1 \leftarrow S_0$	oscillator strengths[b]
ZaZsZa											
PΦB$^+$	2.75	2.72	2.16	2.15	2.18	2.15	2.22	2.19	1.76	1.74	2.32, 2.21, 1.69, 1.65, 1.76, 1.71, 1.31, 1.26
n_APΦB	3.13	2.82	2.73	2.53	2.26	2.17	2.32	2.21	2.40	2.36	2.24, 2.19, 1.58, 1.60, 1.63, 1.65, 1.42, 1.37
n_BPΦB	3.07	2.89	2.78	2.69	2.33	2.28	2.39	2.33	2.43	2.39	2.15, 2.19, 1.42, 1.42, 1.49, 1.50, 1.39, 1.35
n_CPΦB	3.05	2.91	2.69	2.63	2.34	2.33	2.39	2.37	2.30	2.26	2.17, 2.19, 1.42, 1.52, 1.48, 1.56, 1.30, 1.26
n_DPΦB	3.16	2.90	2.46	2.34	2.25	2.22	2.30	2.25	2.11	2.12	1.96, 1.97, 1.20, 1.27, 1.27, 1.34, 1.02, 1.00
ZaZsEa											
PΦB$^+$	2.76	2.72	2.16	2.15	2.20	2.20	2.23	2.23	1.76	1.70	2.30, 2.18, 1.72, 1.66, 1.78, 1.71, 1.28, 1.22
n_APΦB	3.11	2.80	2.70	2.51	2.23	2.13	2.29	2.17	2.39	2.34	2.19, 2.16, 1.48, 1.51, 1.55, 1.58, 1.38, 1.32
n_BPΦB	3.05	2.86	2.75	2.64	2.29	2.22	2.35	2.28	2.42	2.40	2.10, 2.16, 1.31, 1.32, 1.39, 1.40, 1.34, 1.30
n_CPΦB	3.06	2.91	2.71	2.64	2.32	2.32	2.37	2.36	2.35	2.31	2.17, 2.18, 1.31, 1.48, 1.39, 1.53, 1.33, 1.30
n_DPΦB	3.13	2.85	2.49	2.35	2.23	2.21	2.28	2.24	2.15	2.12	1.88, 1.90, 1.16, 1.29, 1.22, 1.34, 1.02, 0.98
ZaZsZs											
PΦB$^+$	2.64	2.55	2.15	2.08	2.10	2.06	2.13	2.09	1.73	1.70	1.06, 0.90, 0.78, 0.66, 0.80, 0.68, 0.64, 0.61
n_APΦB	3.01	2.65	2.66	2.42	2.18	2.05	2.24	2.09	2.33	2.27	0.89, 0.80, 0.73, 0.66, 0.74, 0.67, 0.61, 0.59
n_BPΦB	2.84	2.64	2.57	2.47	2.14	2.07	2.19	2.11	2.19	2.14	0.66, 0.73, 0.45, 0.48, 0.47, 0.49, 0.45, 0.44
n_CPΦB	2.79	2.62	2.45	2.37	2.14	2.11	2.18	2.15	2.06	2.04	0.79, 0.80, 0.50, 0.53, 0.52, 0.54, 0.50, 0.49
n_DPΦB	2.65	2.56	1.99	1.94	2.01	2.00	2.05	2.03	1.85	1.85	0.72, 0.73, 0.42, 0.42, 0.43, 0.43, 0.36, 0.35
ZaZsEs											
PΦB$^+$	2.66	2.56	2.10	2.02	2.11	2.05	2.15	2.09	1.66	1.63	1.22, 1.06, 0.84, 0.70, 0.87, 0.73, 0.69, 0.66
n_APΦB	2.93	2.58	2.57	2.34	2.11	1.97	2.16	2.01	2.25	2.18	0.85, 0.81, 0.62, 0.58, 0.64, 0.59, 0.58, 0.54
n_BPΦB	2.88	2.65	2.59	2.45	2.17	2.07	2.22	2.11	2.24	2.20	0.83, 0.82, 0.51, 0.48, 0.53, 0.50, 0.57, 0.54
n_CPΦB	2.91	2.66	2.56	2.42	2.18	2.10	2.23	2.14	2.20	2.15	0.95, 0.87, 0.53, 0.51, 0.56, 0.53, 0.60, 0.58
n_DPΦB	3.04	2.77	2.34	2.20	2.04	2.04	2.10	2.08	1.92	1.95	1.20, 1.19, 0.51, 0.57, 0.55, 0.61, 0.57, 0.58

[a] Unless otherwise indicated, the 6-31G(d,p) basis set is used. [b] From left to right: CIS and CIS(D) $S_1 \leftarrow S_0$; CIS and CIS(D) $S_1 \rightarrow S_0$; TD-B3LYP $S_1 \leftarrow S_0$; TD-B3LYP $S_1 \rightarrow S_0$; TD-PBE0 $S_1 \leftarrow S_0$; TD-PBE0 $S_1 \rightarrow S_0$; SAC-CI level-1 $S_1 \leftarrow S_0$; SAC-CI level-2 $S_1 \leftarrow S_0$.

TABLE 2: Influence of Basis Set and Implicit Solvation on Vertical Excitation and Emission Energies of *ZaZsZa* Phytochromobilin (in eV)[a]

	6-31G(d,p) gas phase		6-31++G(d,p) gas phase		6-311G(2df,p) gas phase		6-311G(2df,p) IEF-PCM $\epsilon = 4.0$		6-311G(2df,p) IEF-PCM $\epsilon = 78.39$		6-311++G(2df,p) gas phase	
form	$S_1 \leftarrow S_0$	$S_1 \rightarrow S_0$	$S_1 \leftarrow S_0$	$S_1 \rightarrow S_0$	$S_1 \leftarrow S_0$	$S_1 \rightarrow S_0$	$S_1 \leftarrow S_0$	$S_1 \rightarrow S_0$	$S_1 \leftarrow S_0$	$S_1 \rightarrow S_0$	$S_1 \leftarrow S_0$	$S_1 \rightarrow S_0$
PΦB$^+$	2.18	2.15	2.14	2.12	2.16	2.14	2.03	2.00	2.03	2.00	2.14	2.12
n_APΦB	2.26	2.17	2.22	2.12	2.25	2.14	2.08	1.97, 1.94[b]	2.07	1.96	2.22	2.11
n_BPΦB	2.33	2.28	2.29	2.23	2.31	2.25	2.16	2.10	2.16	2.09	2.29	2.23
n_CPΦB	2.34	2.33	2.30	2.29	2.32	2.31	2.14	2.13, 2.02[b]	2.12	2.12	2.29	2.28
n_DPΦB	2.25	2.22	2.19	2.16	2.23	2.19	2.01	1.99, 1.91[b]	1.96	1.97	2.19	2.15

[a] All calculations performed using TD-BLYP. [b] Based on CAS(4,4)/cc-pVDZ S_1 geometries.

energy at the excited-state geometry ($\Delta G^{S_0}_{solv,m}|_{\mathbf{R}=\mathbf{R}(S_1)}$) and a correction term corresponding to the *solvent effect* on the vertical TD-B3LYP energy difference between the two states at the excited-state geometry ($\omega_m^{(S_1-S_0)}|_{\mathbf{R}=\mathbf{R}(S_1)} - \omega_{gas}^{(S_1-S_0)}|_{\mathbf{R}=\mathbf{R}(S_1)}$)[70]

$$\Delta G^{S_1}_{solv,m} \approx \Delta G^{S_0}_{solv,m}|_{\mathbf{R}=\mathbf{R}(S_1)} + \omega_m^{(S_1-S_0)}|_{\mathbf{R}=\mathbf{R}(S_1)} - \omega_{gas}^{(S_1-S_0)}|_{\mathbf{R}=\mathbf{R}(S_1)} \quad (4)$$

In this approach, the solvent is equilibrated to the ground-state charge distribution ("nonequilibrium solvation of the excited state") of the chromophore, which may be a source of error but is likely a reasonable approximation for the present study. First, S_1 is a relatively short-lived excited-state with $Z \rightarrow E$ photoisomerization occurring on a picosecond time scale.[71] Thereby, the solvent representing the protein environment will not have ample time to equilibrate to the excited-state charge distribution. Second, calculation of *relative* pK_a values will reduce the effect of potential errors from this procedure.

Results and Discussion

Photochemistry of PΦB: Performance of Different Methods. Parts of the benchmark calculations are summarized in Tables 1 and 2. The 660 nm absorption maximum of Pr[6] corresponds to a vertical $S_1 \leftarrow S_0$ excitation energy of 1.88 eV. The 672−692 nm fluorescence maximum,[72] in turn, corresponds to a vertical $S_1 \rightarrow S_0$ emission energy of 1.79−1.85 eV. Using gas-phase calculations to assess the performance of the methods and considering first the protonated form of the chromophore, we observe from Table 1 that the SAC-CI excitation energies of *ZaZsZa* PΦB$^+$ (1.76 and 1.74 eV) compare well (~0.1 eV too small) with the experimental value, despite the use of a small basis set. As discussed in a previous section, this particular configuration[11,13,14] and protonation state[11,23−27,30,31] for the Pr chromophore have been implicated in a number of studies. We also note that tightening the thresholds for double-excitation operators from level-1 to level-2 throughout has a small effect (≤0.07 eV). This, of course, is a consequence of S_1 having pronounced single-excitation character.

The CIS(D) (2.16 eV), TD-B3LYP (2.18 eV), and TD-PBE0 (2.22 eV) calculations on *ZaZsZa* PΦB$^+$ are reasonably accurate, overestimating, in contrast to SAC-CI, the experimental value by ~0.3 eV. Furthermore, the accuracy of these methods relative to SAC-CI is not sensitive to which configuration PΦB$^+$ adopts. This suggests that the computational errors introduced by using these more approximate methods are systematic and will largely cancel when relative effects are evaluated.

As expected, the performance of CIS(D) and TD-DFT is markedly better than that of CIS (2.75 eV). Nevertheless, it should be emphasized that CIS theory indeed allows for a qualitatively correct description of singly excited states, and that excitation energies for such states typically are overestimated by 0.5−1.0 eV.[73] This error is primarily due to the use of HF orbitals (virtual HF orbitals are well-known to have too high energies) and the neglect of dynamic electron correlation. The improvement of CIS by CIS(D) (2.75 → 2.16 eV) is a measure of the effect of the latter deficiency, and the difference in CIS(D) (2.16 eV) and SAC-CI (1.76 and 1.74 eV) excitation energies testifies to the magnitude of the former. The better performance of TD-DFT than CIS, in turn, can be attributed to the better agreement between differences in virtual and occupied orbital eigenvalues and exact excitation energies in ground-state DFT than in HF theory, as well as to the inclusion of electron correlation effects by means of an approximate exchange-correlation functional.

Turning to emission energies, the CIS(D) (2.15 eV), TD-B3LYP (2.15 eV), and TD-PBE0 (2.19 eV) calculations on *ZaZsZa* PΦB$^+$ reproduce the 1.79−1.85 eV fluorescence maximum of Pr[72] with an accuracy of ∼0.3−0.4 eV, whereas CIS (2.72 eV) again has a larger error. However, the appreciable improvement over CIS by the other methods clearly suggests that the deficiencies in CIS theory are manifested primarily in the excited-state energy, whereas the predicted geometry should be accurate. Thus, performing CIS(D), TD-B3LYP, or TD-PBE0 single-point calculations on CIS geometries appears to be a fruitful strategy. The calculated Stokes shifts (i.e., differences between vertical excitation and emission energies)—CIS(D) (0.01 eV), TD-B3LYP (0.03 eV), and TD-PBE0 (0.03 eV)—account nicely for the fluorescence of Pr being red-shifted relative to the absorption maximum by 0.03−0.09 eV.[72] Admittedly, this agreement is in part due to cancellation of errors.

As for the neutral forms of the chromophore, the SAC-CI calculations predict a significant absorption blue-shift upon deprotonation of a pyrrolenic nitrogen. Using level-1 thresholds, the average (over the four configurations) blue-shift is 0.62, 0.59, 0.50, and 0.28 eV for ring A, B, C, and D, respectively. A similar effect was recently reported in an experimental study of the gas-phase absorption of the retinal Schiff base chromophore of the rhodopsin photoreceptors.[74] Assuming that the performance of SAC-CI is not sensitive to protonation state, the accuracy of the other methods can be assessed indirectly by using the SAC-CI results as reference data. Including all 16 systems, the following mean and maximum absolute deviations relative to SAC-CI are obtained: CIS (0.76 and 1.12 eV), CIS(D) (0.34 and 0.42 eV), TD-B3LYP (0.10 and 0.16 eV), and TD-PBE0 (0.09 and 0.20 eV). Apparently, the TD-DFT methods are in quite good agreement with SAC-CI and perform better than CIS(D). It should be noted that, albeit of minor importance for reliably computing relative excited-state pK_a's, the deprotonation-induced absorption blue-shifts predicted by TD-B3LYP and TD-PBE0 are much smaller than those predicted by SAC-CI. This discrepancy appears to be due to the combined effect of TD-B3LYP and TD-PBE0 overestimating and SAC-CI slightly underestimating the excitation energies of the protonated species.

Overall, the data in Table 1 seem to suggest that either of the CIS(D), TD-B3LYP and TD-PBE0 methods can be used for qualitatively accurate theoretical studies of the photochemistry of PΦB, in place of much more demanding SAC-CI calculations. Since the TD-B3LYP results are in slightly better agreement with available experimental data than are the TD-PBE0 results, and since TD-DFT methods are less expensive than CIS(D), the excitation energies required for the computation of excited-state pK_a's were obtained by means of TD-B3LYP calculations.

Photochemistry of PΦB: Influence of Basis Set and Implicit Solvation. Table 2 compares vertical TD-B3LYP gas-phase excitation and emission energies of protonated and neutral forms of *ZaZsZa* PΦB calculated with the 6-31G(d,p) double-ζ basis set, a triple-ζ basis set with additional polarization functions (6-311G(2df,p)) and basis sets containing diffuse functions (6-31++G(d,p) and 6-311++G(2df,p)). We observe that using 6-311G(2df,p) instead of 6-31G(d,p) improves the results for PΦB$^+$ with respect to Pr absorption (at 1.88 eV)[6] and fluorescence (at 1.79−1.85 eV)[72] maxima, but that the improvement is small (≤0.02 eV lowering). Similarly, the excitation and emission energies of the neutral forms are lowered by at most 0.03 eV. This observation is in line with the established notion of modest basis set requirements in DFT. Adding diffuse functions to the 6-311G(2df,p) basis set, in turn, results in a further lowering of transition energies by ≤0.04 eV only, which is a consequence of the pronounced valence-excited character of S_1.

Table 2 also compares gas-phase and condensed-phase transition energies. Encouragingly, the use of TD-B3LYP/6-311G(2df,p) in combination with IEF-PCM improves both excitation (2.16 → 2.03 eV) and emission (2.14 → 2.00 eV) energies of PΦB$^+$, and reproduces experimental data with an error of ∼0.1−0.2 eV only. This holds true for both values of the dielectric constant. In analogy with the situation in the gas phase, additional computations showed that IEF-PCM transition energies are not sensitive to the choice of basis set. On the basis of the data in Table 2, the TD-B3LYP-IEF-PCM excited-state pK_a calculations were carried out with the 6-311G(2df,p) basis set and the dielectric constant set to 4.0 (representing a protein environment).

To further evaluate the quality of CIS excited-state geometries and estimate the error introduced by neglecting nondynamic electron correlation, TD-B3LYP-IEF-PCM/6-311G(2df,p) emission energies were also calculated on the basis of CASSCF geometries. Although CASSCF(4,4)/cc-pVDZ excited-state geometry optimizations were attempted for all five forms of *ZaZsZa* PΦB, they were feasible only for n_APΦB, n_CPΦB, and n_DPΦB. Nevertheless, comparing the emission energies computed at the resulting structures with those at the corresponding CIS structures (Table 2) shows that the geometric effect amounts to 0.03 (n_APΦB), 0.11 (n_CPΦB), and 0.08 eV (n_DPΦB) only. This indicates that there are no near-degeneracy effects to warrant a (much more expensive) multi-reference treatment.

As to the effect of dynamic electron correlation on excited-state geometries, Table 3 compares CIS structures of *ZaZsZa* PΦB$^+$ and n_BPΦB with structures obtained by performing TD-B3LYP/SVP and SAC-CI/6-31G excited-state geometry optimizations. Calculated TD-B3LYP-IEF-PCM/6-311G(2df,p) emission energies on the optimized structures are also listed. For both forms, the CIS/SVP and CIS/6-31G bond lengths are in good agreement with the respective TD-B3LYP and SAC-CI values, deviating on average by <0.02 and <0.01 Å only. Accordingly, the improvement in PΦB$^+$ emission energies from using TD-B3LYP (2.02 → 1.91 eV) or SAC-CI (2.01 → 1.99 eV) instead of CIS geometries is relatively minor.

TABLE 3: Optimized CIS, TD-B3LYP and SAC-CI Excited-State (S_1) Geometric Parameters (in Å and Degrees) of *ZaZsZa* PΦB$^+$ and n_BPΦB, and Influence of Excited-State Geometry on Vertical Emission Energy ($\Delta E(S_1 \rightarrow S_0)$, in eV)

	CIS/6-31G(d,p)		CIS/SVP		TD-B3LYP/SVP		CIS/6-31G		SAC-CI/6-31G	
	PΦB$^+$	n_BPΦB	PΦB$^+$	n_BPΦB	PΦB$^+$	n_BPΦB	PΦB$^+$	n_BPΦB	PΦB$^+$	n_BPΦB
C1−C2	1.513	1.516	1.512	1.516	1.523	1.527	1.508	1.511	1.508	1.512
C1−N(A)	1.394	1.370	1.396	1.373	1.414	1.396	1.393	1.371	1.400	1.377
C1−O1	1.181	1.191	1.176	1.185	1.199	1.206	1.208	1.217	1.212	1.223
C2−C3	1.536	1.536	1.533	1.533	1.539	1.540	1.540	1.540	1.542	1.543
C3−C4	1.517	1.517	1.516	1.517	1.519	1.519	1.519	1.520	1.517	1.518
C4−N(A)	1.354	1.383	1.352	1.381	1.362	1.376	1.362	1.389	1.364	1.392
C4−C5	1.359	1.339	1.363	1.344	1.379	1.372	1.360	1.342	1.363	1.347
C5−C6	1.421	1.443	1.423	1.445	1.420	1.435	1.419	1.435	1.420	1.436
C6−C7	1.411	1.452	1.415	1.455	1.432	1.443	1.415	1.453	1.413	1.446
C6−N(B)	1.367	1.321	1.366	1.320	1.380	1.362	1.376	1.337	1.378	1.346
C7−C8	1.375	1.352	1.377	1.355	1.381	1.381	1.379	1.359	1.386	1.370
C8−C9	1.412	1.445	1.416	1.448	1.437	1.443	1.415	1.447	1.412	1.434
C9−N(B)	1.386	1.362	1.384	1.359	1.399	1.363	1.393	1.376	1.394	1.378
C9−C10	1.393	1.394	1.397	1.399	1.385	1.425	1.393	1.392	1.401	1.406
C10−C11	1.393	1.393	1.397	1.397	1.437	1.388	1.393	1.392	1.398	1.390
C11−C12	1.415	1.424	1.419	1.427	1.407	1.434	1.419	1.427	1.419	1.431
C11−N(C)	1.384	1.366	1.381	1.365	1.384	1.390	1.389	1.374	1.392	1.379
C12−C13	1.371	1.364	1.373	1.367	1.408	1.380	1.374	1.368	1.379	1.368
C13−C14	1.414	1.428	1.419	1.432	1.406	1.446	1.419	1.433	1.422	1.443
C14−N(C)	1.376	1.359	1.374	1.358	1.391	1.362	1.384	1.368	1.385	1.360
C14−C15	1.408	1.407	1.411	1.410	1.434	1.419	1.404	1.403	1.403	1.404
C15−C16	1.369	1.367	1.374	1.371	1.379	1.390	1.372	1.370	1.380	1.376
C16−C17	1.447	1.438	1.450	1.441	1.446	1.441	1.447	1.439	1.440	1.438
C16−N(D)	1.368	1.381	1.366	1.379	1.384	1.383	1.377	1.388	1.376	1.384
C17−C18	1.344	1.350	1.347	1.354	1.378	1.382	1.352	1.358	1.364	1.368
C18−C19	1.505	1.491	1.507	1.494	1.509	1.493	1.498	1.483	1.503	1.490
C19−N(D)	1.392	1.384	1.392	1.384	1.400	1.408	1.392	1.385	1.397	1.394
C19−O19	1.185	1.195	1.179	1.189	1.210	1.217	1.212	1.224	1.214	1.224
C18−C18^1	1.452	1.454	1.454	1.456	1.438	1.445	1.445	1.449	1.442	1.446
C18^1−C18^2	1.328	1.327	1.332	1.331	1.360	1.351	1.334	1.333	1.346	1.345
N(A)−C4−C5−C6	−4.9	−3.3	−4.2	−3.1	−4.4	−3.4	−5.0	−3.6	−5.0	−3.7
C4−C5−C6−C7	−17.1	−19.0	−14.7	−17.0	−10.9	−11.5	−15.3	−16.3	−15.3	−17.2
N(B)−C9−C10−C11	11.8	−0.3	12.5	−0.3	7.5	−1.0	14.1	−0.2	11.5	−0.1
C9−C10−C11−C12	−168.0	179.8	−167.8	179.9	−158.1	180.0	−167.0	179.9	−167.7	179.4
N(C)−C14−C15−C16	168.8	170.8	169.9	172.2	166.9	170.4	170.4	173.8	167.4	167.8
C14−C15−C16−C17	174.3	174.2	175.1	175.1	175.6	174.5	175.1	175.9	174.7	175.6
rms deviation			0.018[a]	0.018[a]			0.005[b]	0.007[b]		
maximum deviation			0.040[a]	0.042[a]			0.012[b]	0.014[b]		
$\Delta E(S_1 \rightarrow S_0)$[c]	2.00	2.10	2.02	2.08	1.91	1.96	2.01	2.06	1.99	2.01

[a] Root-mean-square and maximum absolute deviation (in Å) of CIS/SVP bond lengths relative to TD-B3LYP/SVP. [b] Root-mean-square and maximum absolute deviation (in Å) of CIS/6-31G bond lengths relative to SAC-CI/6-31G. [c] TD-B3LYP-IEF-PCM/6-311G(2df,p) single-point calculations with $\epsilon = 4.0$.

Of course, given that TD-DFT methods in general yield better excited-state geometries than CIS but have similar computational requirements, one may legitimately argue that TD-B3LYP should anyhow be the preferred method for geometry optimization. However, to estimate pK_a values quantum chemically, it is imperative to compute vibrational frequencies for extracting free energies. For systems the size of PΦB, this is only feasible provided that analytic force constants are available. While CIS fulfills this criterion, TD-DFT methods (and SAC-CI) do not. Furthermore, the benchmark calculations clearly suggest that CIS is indeed a reliable method for locating minima on the S_1 potential-energy surface of PΦB.

Ground- and Excited-State Acidity of PΦB. The calculated relative pK_a values of *ZaZsZa*, *ZaZsEa*, *ZaZsZs*, and *ZaZsEs* PΦB$^+$ are presented in Figure 2, using ground and excited-state deprotonation of the A-ring nitrogen of *ZaZsZa* PΦB$^+$ as reference reactions (with $\Delta pK_a^{S_0} = 0$ and $\Delta pK_a^{S_1} = 0$). Rings and configurations predicted to be more acidic have (cf. eq 3) *negative* ΔpK_a values. Figure 2 also shows calculated ground and excited-state proton affinities (PA) of the *neutral* PΦB forms, given relative to the respective PA of *ZaZsZa* n_APΦB. PA is a gas-phase property given in terms of enthalpies as

$$PA^I(n_X P\Phi B) = -[H^I_{gas}(P\Phi B^+) - H^I_{gas}(n_X P\Phi B) - 5RT/2] \quad (5)$$

In accordance with the pK_a calculations, the PAs were obtained at the B3LYP/6-311G(2df,p)//B3LYP/6-31G(d,p) (S_0) and TD-B3LYP/6-311G(2df,p)//CIS/6-31G(d,p) (S_1) levels of theory. Pyrrole moieties and chromophore configurations more prone to lose a proton than A and *ZaZsZa* have negative ΔPAs.

Ground- and Excited-State Acidity of PΦB: Different Moieties and Effect of Partial Bond Rotations. Considering first the electronic ground state, rings B and C are predicted to be the strongest acids, with pK_a values 4−6 units below that of A. Indeed, B and C are the moieties that have been implicated in studies favoring the possibility of a change in protonation state during the photoactivation.[23,24] The calculated PAs indicate that B and C are the strongest acids (by 10−16 kcal mol^{-1} over A) also in the gas phase. In fact, by means of a regression analysis, the dependence of ΔpK_a on ΔPA was shown to quite

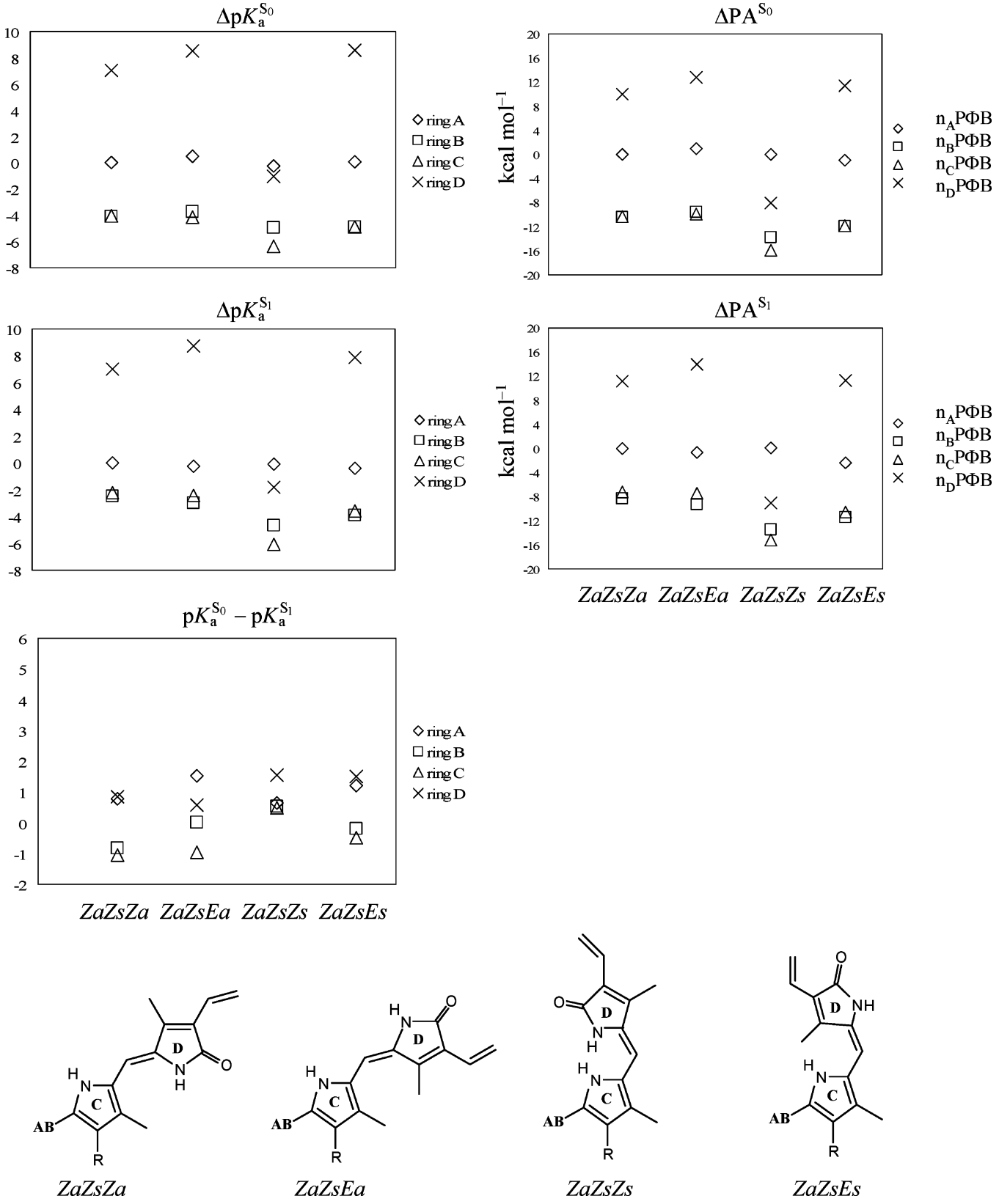

Figure 2. Left panels: relative ($\Delta pK_a^{S_0}$ and $\Delta pK_a^{S_1}$) and difference in absolute ($pK_a^{S_0} - pK_a^{S_1}$) ground and excited-state pK_a values of $P\Phi B^+$. Right panels: relative ground and excited-state proton affinities (ΔPA^{S_0} and ΔPA^{S_1}) of $n_XP\Phi B$.

closely follow a linear relationship (correlation coefficient ~0.984 for the 16 (ΔpK_a, ΔPA) data points). This suggests that the relative pK_a's are governed primarily by differences in the PAs of the neutral species, rather than by differences in how the rings are solvated by the bulk medium.

Turning to the excited-state pK_a's, the pattern is very similar. Hence, B and C are predicted to remain the strongest acids even after electronic excitation. Arguably, this finding is related to the local (rather than charge transfer) character of the excitation. The acidity of B and C relative to A is somewhat smaller (2−6

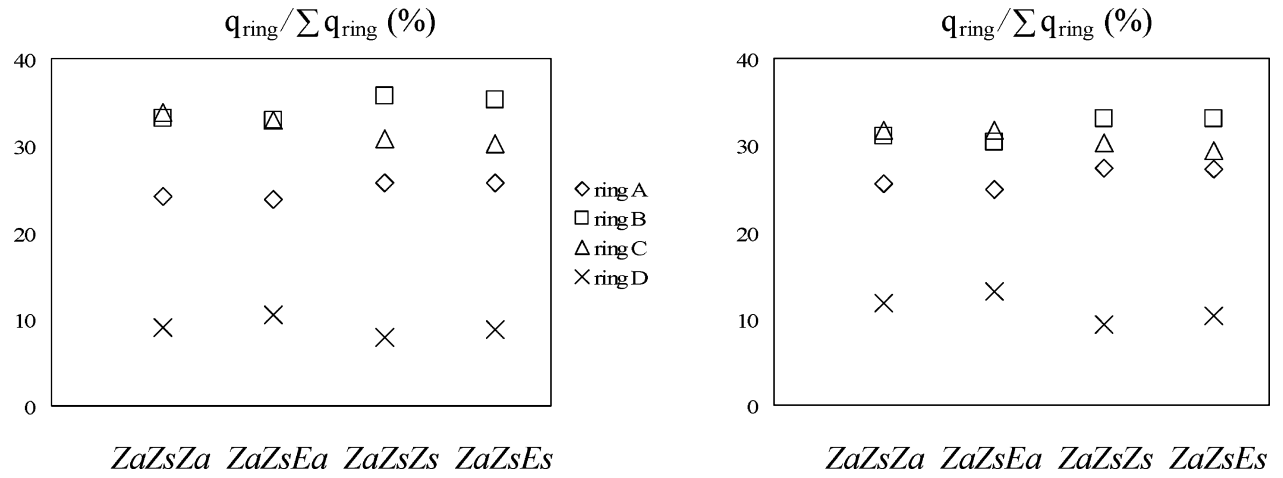

Figure 3. Distribution of positive charge between pyrrole rings in the ground state of PΦB$^+$. Left panel: B3LYP-IEF-PCM/6-311G(2df,p), ϵ = 4.0. Right panel: B3LYP/6-311G(2df,p).

pK_a units) than in the ground state (4−6 pK_a units). As for the dependence of $\Delta pK_a^{S_1}$ on ΔPA^{S_1}, a linear regression analysis indicates (correlation coefficient ~0.987) that differences in PAs are the primary source also for the differences in excited-state pK_a's.

The greater acidity of rings B and C can partly be explained by the distribution of the positive charge between the pyrrole moieties of PΦB$^+$. This is shown in Figure 3, for the electronic ground state. Accordingly, B and C carry a larger portion (30−36% each using IEF-PCM) of the positive charge than A (24−26%) and D (8−10%), which of course tends to increase the acidity. The distribution is similar, albeit with slightly less pronounced differences between the rings, in the gas phase. Although computed charge distributions can be strongly dependent on the quantum chemical method employed (here B3LYP), basis-set size (6-311G(2df,p)), and scheme used for population analysis (Mulliken), additional calculations showed that the results of Figure 3 are not sensitive in this regard.

Intramolecular interactions are also a major factor contributing to the greater acidity of rings B and C. In particular, given a *Z,syn* geometry of the BC methine bridge, deprotonation of these rings is favored by the stabilization of n_BPΦB and n_CPΦB by hydrogen bonds (Figure 4). Similarly, while D is by far the least acidic moiety of *ZaZsZa*, *ZaZsEa*, and *ZaZsEs* PΦB$^+$ (7−9 units higher pK_a than A), in *ZaZsZs* PΦB$^+$ it is actually slightly more acidic than A due to intramolecular hydrogen bonding. Obviously, a *ZaZsZs* configuration also allows for additional stabilization of n_BPΦB and n_CPΦB, which is reflected in the maximum acidity of B and C at this geometry.

So far, we have focused on pK_a values computed using potential-energy minimum structures of PΦB$^+$ and n_XPΦB. This procedure allows for an unbiased assessment of the relative intrinsic acidities of different pyrrole moieties and chromophore configurations, which is the overriding goal of this work. However, in a protein-bound state, the chromophore may experience forces populating other conformations than potential-energy minima. It is therefore of interest to examine the effect of partial bond rotations about the methine bridges on pK_a's. To this end, relative ground-state pK_a's of torsionally distorted *ZaZsZa* PΦB$^+$ were computed. Relevant structures were obtained by performing constrained geometry optimizations with the dihedral angles of the AB, BC, and CD methine bridges held fixed at 0, 15, 30, and 45° deviation from planarity. The results are shown in Figure 5, which displays the *change* in ΔpK_a ($\Delta\Delta pK_a$) relative to that computed using potential-energy minimum structures of *ZaZsZa* PΦB$^+$ and n_XPΦB.

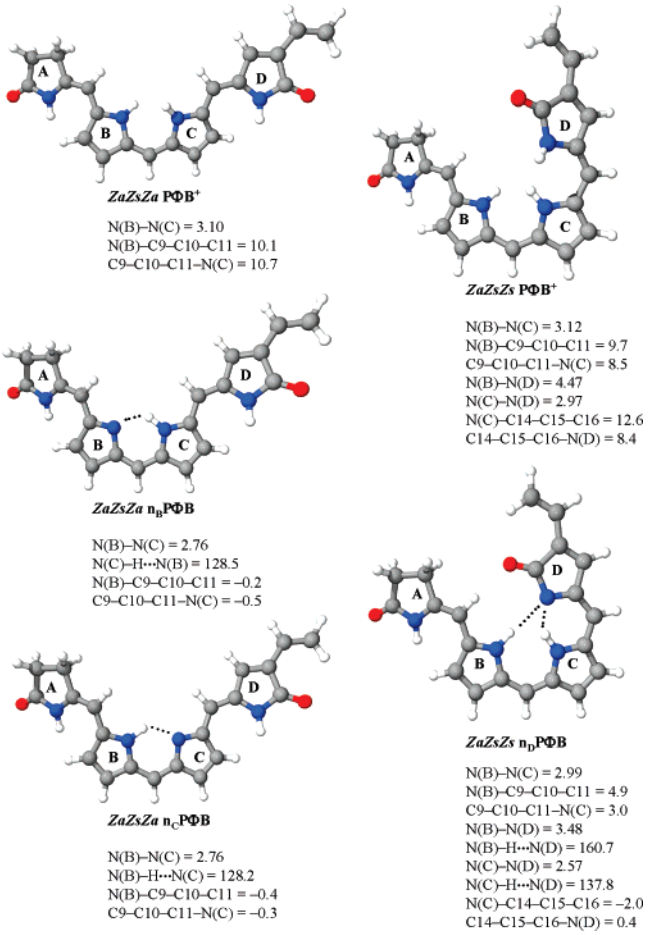

Figure 4. Optimized structures of protonated and neutral forms of *ZaZsZa* and *ZaZsZs* PΦB showing the stabilization of the neutral forms by intramolecular hydrogen bonds (geometric parameters in Å and degrees).

For rings A and D, we observe that ≤30° rotation about the AB and CD methine bridges, respectively, changes the acidities by at most 2 pK_a units. Considering further rotation (≤45°), the effect is more pronounced. For A, the maximum increase ($\Delta\Delta pK_a \sim -4$) and the maximum decrease ($\Delta\Delta pK_a \sim 4$) in acidity amount to 4 pK_a units. For D, the maximum increase is 5 and the maximum decrease is 4 pK_a units. Clearly, if PΦB$^+$ adopts a conformation about these bridges that is much more (*less*) distorted relative to the PΦB$^+$ potential-energy minimum than the neutral forms are distorted relative to the their potential-

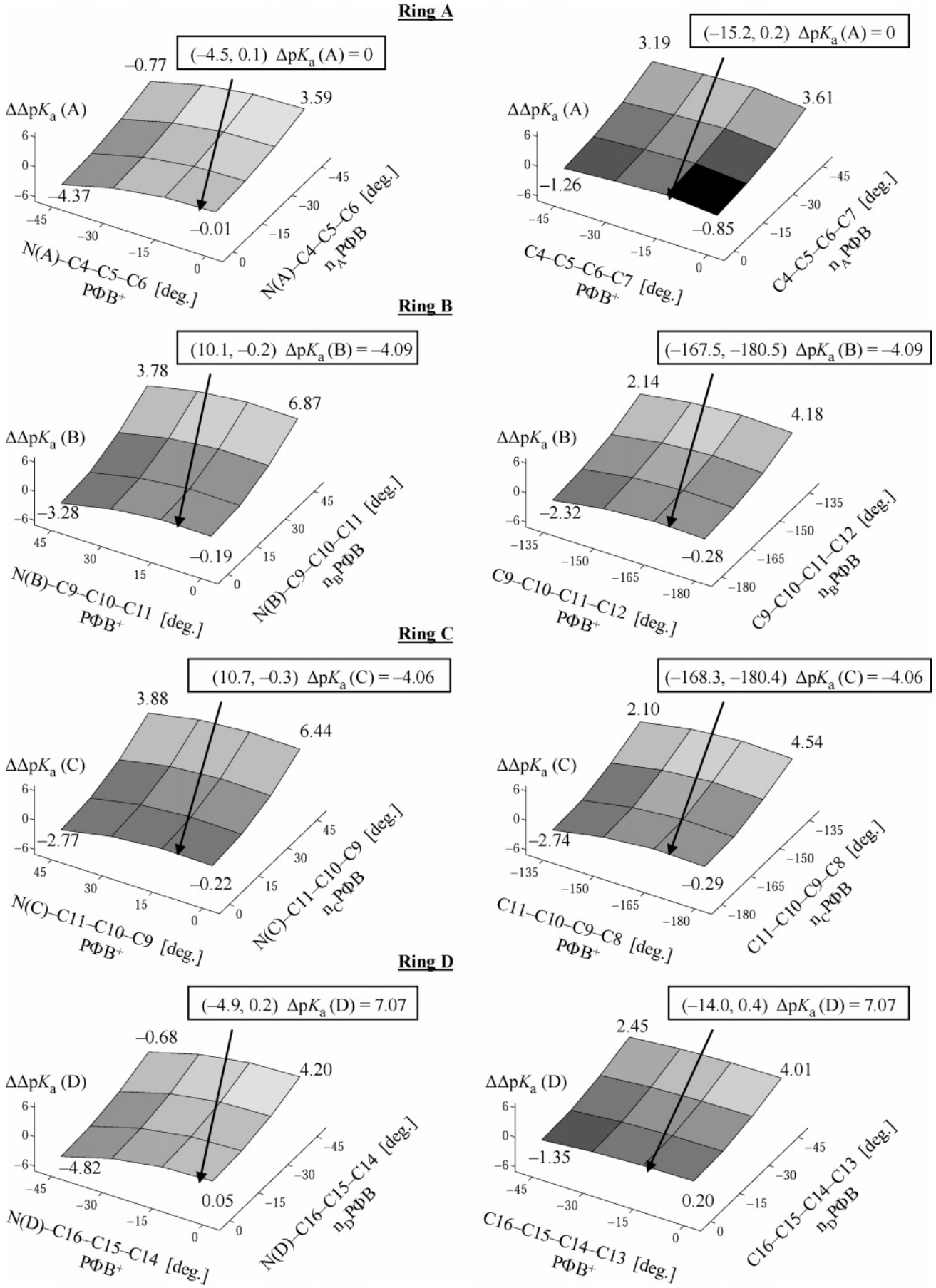

Figure 5. Effect of partial bond rotations about methine bridges on relative ground-state pK_a values of PΦB$^+$. ΔΔpK_a denotes the change in ΔpK_a value relative to that computed using potential-energy minimum structures of *ZaZsZa* PΦB$^+$ and n_XPΦB. The dihedral angles of potential-energy minima are indicated by arrows, with the corresponding values and reference ΔpK_a given explicitly in the boxes.

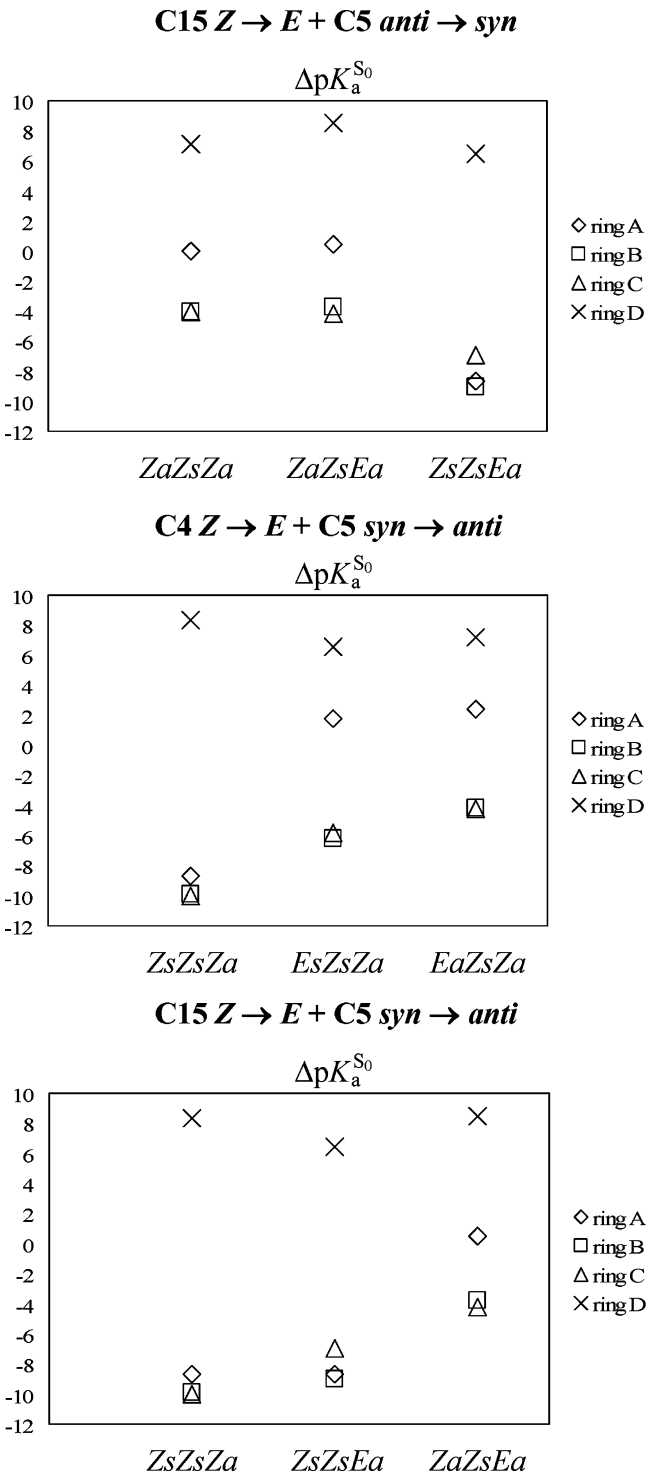

Figure 6. Effect of isomerization reactions comprising a thermal single-bond rotation at C5 on relative ground-state pK_a values of PΦB$^+$.

energy minima, the acidities of A and D increase (*decrease*). This is because such a conformational difference favors (*disfavors*) the Gibbs free-energy change of deprotonation. Thus, the protein may tune the pK_a values in a protein-bound state by exerting torsional strain that differ in magnitude between PΦB$^+$ and n_XPΦB. As for partial bond rotations about the BC methine bridges and their influence on the pK_a's of rings B and C, the situation is very similar. Note, however, that rotations of n_BPΦB about C9−C10 and n_CPΦB about C10−C11 have a particularly strong tendency to decrease the acidities of B and C. This is because these rotations break the N(C)−H···N(B) and N(B)−H···(C) intramolecular hydrogen bonds.

Ground- and Excited-State Acidity of PΦB: Effect of Isomerization and Light Absorption. Having dealt with relative acidities of the different pyrrole moieties and the effect of partial bond rotations, we now turn to discussing whether isomerization and/or light absorption facilitate a proton transfer. As for the first issue, assuming a *ZaZsZa* configuration for the Pr chromophore[11,13,14] and considering first a sole C15 $Z \rightarrow E$ double-bond isomerization (*ZaZsZa* → *ZaZsEa*),[3,4,15,17] there are no signs (Figure 2) that this reaction entails an appreciable increase in the acidities of the pyrrole moieties. This holds true for both the ground state ($-0.1 < \Delta\Delta pK_a^{S_0}(\text{iso}) < 1.5$) and the excited state ($-0.5 < \Delta\Delta pK_a^{S_1}(\text{iso}) < 1.8$). Including an additional C15 single-bond rotation event[10,12] (*ZaZsZa* → *ZaZsEs*) in the analysis one arrives at the same conclusion, although B and C are slightly more acidic in the *ZaZsEs* configuration than in *ZaZsEa* (ground state, $-0.9 < \Delta\Delta pK_a^{S_0}(\text{iso}) < 1.6$; excited state, $-1.5 < \Delta\Delta pK_a^{S_1}(\text{iso}) < 0.9$).

To investigate whether light absorption increases the acidity of PΦB$^+$ relative to the ground state, and to assess whether a photochemical (rather than thermal) deprotonation of the chromophore can be expected simply because an excited-state proton transfer is more favorable than a ground-state process in Pr, differences in *absolute* ground and excited-state pK_a's were calculated as well. Using eq 2, these were obtained as

$$pK_a^{S_0} - pK_a^{S_1} = [\Delta G_m^{S_1-S_0}(\text{P}\Phi\text{B}^+) - \Delta G_m^{S_1-S_0}(n_X\text{P}\Phi\text{B})]/RT \ln 10 \quad (6)$$

where $\Delta G_m^{S_1-S_0} = G_m^{S_1} - G_m^{S_0}$ denotes the free-energy difference between the S_0 and S_1 states. Overall, the calculations (Figure 2) are not indicative of any significant difference in acidity between the two states. In fact, the maximum $pK_a^{S_0}$ - $pK_a^{S_1}$ values for rings B and C amount to 0.5 only. It should be pointed out that the use of B3LYP S_0 and CIS S_1 geometries may introduce a certain degree of ambiguity upon *explicit* comparison between ground and excited-state pK_a's. On the other hand, the accuracy of the TD-B3LYP Stokes shifts seems to justify such a procedure, as the corresponding calculations involve a similar type of comparison.

The field of acid−base chemistry of excited states has its origin in the work by Förster[75] and Weller,[76] with several reviews appearing in more recent years.[77−80] With knowledge of the ground-state pK_a of an acid HA, the excited-state pK_a can be estimated by measuring the absorption or emission spectra (rather than the free-energy differences of the states) of HA and its conjugate base A^-. The corresponding form of eq 6 is commonly known as the Förster equation. Accordingly, it is predicted that the excited state is more acidic than the ground state if the spectrum of A^- is red-shifted relative to the spectrum of HA. However, as seen in a previous section (Tables 1 and 2), the excitation and emission energies of n_XPΦB are, in fact, blue-shifted relative to PΦB$^+$. This observation strengthens the prediction that the excited state is no more acidic than the ground state. Qualitatively, the magnitude of the blue-shifts ($\leq$0.13 eV for all rings at the level of theory used for the pK_a calculations) is consistent with the small $pK_a^{S_0} - pK_a^{S_1}$ values reported in Figure 2.[81] Future computational studies may therefore identify particular PΦB configurations exhibiting a pronounced difference in ground- and excited-state pK_a's by direct calculation of spectroscopic parameters, rather than by explicit calculation of pK_a values.

In summary, given a protonated[11,23−27,30,31] *ZaZsZa*[11,13,14] chromophore in its ground state in Pr, the calculations suggest that neither isomerization at C15 nor promotion of the system

to an excited-state potential-energy surface facilitates a proton transfer. Consequently, in the absence of chromophore−protein interactions substantially different from those in Pr with regard to influence on pK_a values, the study supports the notion that the chromophore remains protonated during the photoactivation and predicts that any proton-transfer event in a subsequent state would have to be due to altered interactions with the protein in that state.

As to the effect of isomerization at C5 on pK_a values, the corresponding calculations are summarized in Figure 6. Excited-state pK_a's are not presented, since these (again) were found to be very similar to the ground-state pK_a's. Three different isomerization pathways were considered. For the first[13] (top panel), we observe that a full *anti* → *syn* rotation at C5 results in an appreciable lowering of the pK_a's of A (by 9 units), B (5), and C (3), as the A-ring nitrogen thereby can form hydrogen bonds with the nitrogens of B and C. Thus, the *partial* C5 *anti* → *syn* rotation proposed by Mroginski et al.[13] may well increase the propensity of PΦB$^+$ to release its excess proton to the protein. Note, however, that tight packing of these moieties by the protein has been put forth as an argument against rotations at C5 and C10.[3,4] Obviously, for the second[18] (middle panel) and third[19] (bottom) pathways it is similarly clear that a Pr *ZsZsZa* configuration favors intramolecular hydrogen bonding. Accordingly, the pK_a values of A, B, and C inevitably increase when the chromophore isomerizes at C4 or C5. Hence, these pathways do not facilitate a proton-transfer reaction.

Although there are 64 possible isomers of PΦB, it is important to point out that we are herein exclusively concerned with isomers implicated by experiments, and that there are a number of alternative isomerization pathways that have not been addressed. To the best of our knowledge, however, all pathways actually discussed in the literature are covered by the present calculations. Still, since definite assignments of PΦB geometry in different states along the Pr → Pfr reaction cycle are yet to appear, it is clear that theoretical assessment of alternative pathways is a worthwhile objective for future studies.

The ultimate goal of computational studies of the present type is to include also the surrounding protein in the modeling. For example, the Pr bacteriophytochrome X-ray structure identified two amino acid residues (Asp207 and His260) well-suited and appropriately positioned to function as proton donors for the BC dipyrrolic moiety.[15] These residues should stabilize the positive charge of the Pr chromophore and increase its pK_a's. A key question for future experimental and theoretical studies is therefore the possibility that these interactions are disrupted in subsequent states, yielding a more acidic chromophore.

Conclusions

The photoactivation of the plant photoreceptor phytochrome is governed by a red-light induced *Z* → *E* photoisomerization of its PΦB chromophore. In this work, relative ground (S_0) and excited-state (S_1) pK_a values of the different pyrrole rings of PΦB are calculated by means of quantum chemical methods, with the aim to shed new light on the controversial issue that a proton transfer may occur from the chromophore to the surrounding protein during the photoactivation. In particular, we have investigated whether the basic events of the photoactivation (i.e., light absorption and chromophore isomerization) facilitates a proton transfer by increasing the *intrinsic* acidity of PΦB.

Focusing on configurations produced by isomerizations at C15[3,4,10,12,15,17] of a Pr *ZaZsZa*[11,13,14] chromophore and performing calculations at a carefully calibrated level of theory, it is shown that rings B and C are the strongest acids both in the ground state (by 4−6 pK_a units over A) and the excited state (by 2−6 pK_a units over A). This feature is consistent with the observation that B and C are the moieties possibly involved in proton transfer[23,24] and can be rationalized in terms of the distribution of the net positive charge in the parent PΦB$^+$ species, and by the extent to which the neutral n_XPΦB forms are stabilized by intramolecular hydrogen bonding.

Furthermore, it is demonstrated that neither C15 *Z,anti* → *E,anti*[3,4,15,17] nor C15 *Z,anti* → *E,syn*[10,12] isomerization lowers the pK_a values. As to the effect of light absorption on acidity, it is found by computing differences in absolute ground and excited-state pK_a's that the excited-state is no more acidic than the ground state, which is also confirmed by a Förster-type analysis of shifts in excitation and emission energies of n_XPΦB relative to PΦB$^+$. Given a protonated species in its ground state in Pr,[11,23−27,30,31] it is thereby suggested that the chromophore from the point of view of its intrinsic acidity remains protonated during the photoactivation and argued that any proton-transfer reaction in a state following Pr can only be brought about by a protein-induced lowering of the relevant pK_a.

Acknowledgment. B.D. acknowledges financial support from the Swedish Research Council (VR). O.A.B acknowledges Sten Lunell for support and for making computational resources at UPPMAX and NSC available for this project.

Supporting Information Available: Optimized geometries and energies of structures discussed in the text and complete citation for ref 50. This material is available free of charge via the Internet at http://pubs.acs.org.

References and Notes

(1) Pratt, L. H. *Photochem. Photobiol.* **1995**, *61*, 10.
(2) Quail, P. H.; Boylan, M. T.; Parks, B. M.; Short, T. W.; Xu, Y.; Wagner, D. *Science* **1995**, *268*, 675.
(3) Rockwell, N. C.; Su, Y.-S.; Lagarias, J. C. *Annu. Rev. Plant Biol.* **2006**, *57*, 837.
(4) Rockwell, N. C.; Lagarias, J. C. *Plant Cell* **2006**, *18*, 4.
(5) Karniol, B.; Wagner, J. R.; Walker, J. M.; Vierstra, R. D. *Biochem. J.* **2005**, *392*, 103.
(6) Rüdiger, W.; Thümmler, F. *Angew. Chem., Int. Ed. Engl.* **1991**, *30*, 1216.
(7) Lagarias, J. C.; Rapoport, H. *J. Am. Chem. Soc.* **1980**, *102*, 4821.
(8) Rüdiger, W.; Thümmler, F.; Cmiel, E.; Schneider, S. *Proc. Natl. Acad. Sci. U.S.A.* **1983**, *80*, 6244.
(9) Fodor, S. P. A.; Lagarias, J. C.; Mathies, R. A. *Biochemistry* **1990**, *29*, 11141.
(10) Andel, F., III; Lagarias, J. C.; Mathies, R. A. *Biochemistry* **1996**, *35*, 15997.
(11) Kneip, C.; Hildebrandt, P.; Schlamann, W.; Braslavsky, S. E.; Mark, F.; Schaffner, K. *Biochemistry* **1999**, *38*, 15185.
(12) Andel, F., III; Murphy, J. T.; Haas, J. A.; McDowell, M. T.; van der Hoef, I.; Lugtenburg, J.; Lagarias, J. C.; Mathies, R. A. *Biochemistry* **2000**, *39*, 2667.
(13) Mroginski, M. A.; Murgida, D. H.; von Stetten, D.; Kneip, C.; Mark, F.; Hildebrandt, P. *J. Am. Chem. Soc.* **2004**, *126*, 16734.
(14) Hasegawa, J.; Isshiki, M.; Fujimoto, K.; Nakatsuji, H. *Chem. Phys. Lett.* **2005**, *410*, 90.
(15) Wagner, J. R.; Brunzelle, J. S.; Forest, K. T.; Vierstra, R. D. *Nature* **2005**, *438*, 325.
(16) Evans, K.; Grossmann, J. G.; Fordham-Skelton, A. P.; Papiz, M. Z. *J. Mol. Biol.* **2006**, *364*, 655.
(17) Inomata, K.; Hammam, M. A. S.; Kinoshita, H.; Murata, Y.; Khawn, H.; Noack, S.; Michael, N.; Lamparter, T. *J. Biol. Chem.* **2005**, *280*, 24491.
(18) van Thor, J. J.; Mackeen, M.; Kuprov, I.; Dwek, R. A.; Wormald, M. R. *Biophys. J.* **2006**, *91*, 1811.
(19) van Thor, J. J.; Ronayne, K. L.; Towrie, M. *J. Am. Chem. Soc.* **2007**, *129*, 126.
(20) Hoff, W. D.; Jung, K.-H.; Spudich, J. L. *Annu. Rev. Biophys. Biomol. Struct.* **1997**, *26*, 223.

(21) Spudich, J. L.; Yang, C.-S.; Jung, K.-H.; Spudich, E. N. *Annu. Rev. Cell. Dev. Biol.* **2000**, *16*, 365.
(22) van der Horst, M. A.; Hellingwerf, K. J. *Acc. Chem. Res.* **2004**, *37*, 13.
(23) Mizutani, Y.; Tokutomi, S.; Aoyagi, K.; Horitsu, K.; Kitagawa, T. *Biochemistry* **1991**, *30*, 10693.
(24) Mizutani, Y.; Tokutomi, S.; Kitagawa, T. *Biochemistry* **1994**, *33*, 153.
(25) Matysik, J.; Hildebrandt, P.; Schlamann, W.; Braslavsky, S. E.; Schaffner, K. *Biochemistry* **1995**, *34*, 10497.
(26) Foerstendorf, H.; Mummert, E.; Schäfer, E.; Scheer, H.; Siebert, F. *Biochemistry* **1996**, *35*, 10793.
(27) Foerstendorf, H.; Benda, C.; Gärtner, W.; Storf, M.; Scheer, H.; Siebert, F. *Biochemistry* **2001**, *40*, 14952.
(28) van Thor, J. J.; Borucki, B.; Crielaard, W.; Otto, H.; Lamparter, T.; Hughes, J.; Hellingwerf, K. J.; Heyn, M. P. *Biochemistry* **2001**, *40*, 11460.
(29) Borucki, B.; von Stetten, D.; Seibeck, S.; Lamparter, T.; Michael, N.; Mroginski, M. A.; Otto, H.; Murgida, D. H.; Heyn, M. P.; Hildebrandt, P. *J. Biol. Chem.* **2005**, *280*, 34358.
(30) Strauss, H. M.; Hughes, J.; Schmieder, P. *Biochemistry* **2005**, *44*, 8244.
(31) Rohmer, T.; Strauss, H.; Hughes, J.; de Groot, H.; Gärtner, W.; Schmieder, P.; Matysik, J. *J. Phys. Chem. B* **2006**, *110*, 20580.
(32) Durbeej, B.; Borg, O. A.; Eriksson, L. A. *Phys. Chem. Chem. Phys.* **2004**, *6*, 5066.
(33) Durbeej, B.; Borg, O. A.; Eriksson, L. A. *Chem. Phys. Lett.* **2005**, *416*, 83.
(34) Durbeej, B.; Eriksson, L. A. *Phys. Chem. Chem. Phys.* **2006**, *8*, 4053.
(35) Head-Gordon, M.; Rico, R. J.; Oumi, M.; Lee, T. J. *Chem. Phys. Lett.* **1994**, *219*, 21.
(36) Nakatsuji, H. *Chem. Phys. Lett.* **1978**, *59*, 362.
(37) Nakatsuji, H. In *Computational Chemistry: Reviews of Current Trends*; Leszczynski, J., Ed.; Vol. 2; World Scientific: Singapore, 1997; p 62.
(38) Adamo, C.; Barone, V. *J. Chem. Phys.* **1999**, *110*, 6158.
(39) Casida, M. E. In *Recent Advances in Density Functional Methods, Part I*; Chong, D. P., Ed.; World Scientific: Singapore, 1995; p 155.
(40) Bauernschmitt, R.; Ahlrichs, R. *Chem. Phys. Lett.* **1996**, *256*, 454.
(41) Stratmann, R. E.; Scuseria, G. E.; Frisch, M. J. *J. Chem. Phys.* **1998**, *109*, 8218.
(42) Marques, M. A. L.; Gross, E. K. U. *Annu. Rev. Phys. Chem.* **2004**, *55*, 427.
(43) Cancès, E.; Mennucci, B.; Tomasi, J. *J. Chem. Phys.* **1997**, *107*, 3032.
(44) Tomasi, J.; Mennucci, B.; Cammi, R. *Chem. Rev.* **2005**, *105*, 2999.
(45) Roos, B. O. In *Ab Initio Methods in Quantum Chemistry*; Lawley, K. P., Ed.; Wiley: New York, 1987; Part II, p 399.
(46) Roos, B. O. *Adv. Chem. Phys.* **1987**, *69*, 399.
(47) Furche, F.; Ahlrichs, R. *J. Chem. Phys.* **2002**, *117*, 7433.
(48) Dunning, T. H., Jr. *J. Chem. Phys.* **1989**, *90*, 1007.
(49) Schäfer, A.; Horn, H.; Ahlrichs, R. *J. Chem. Phys.* **1992**, *97*, 2571.
(50) Frisch, M. J.; et al. *Gaussian 03*, revision D.01; Gaussian, Inc.: Wallingford, CT, 2004.
(51) Karlström, G.; Lindh, R.; Malmqvist, P.-Å.; Roos, B. O.; Ryde, U.; Veryazov, V.; Widmark, P.-O.; Cossi, M.; Schimmelpfennig, B.; Neogrady, P.; Seijo, L. *Comput. Mater. Sci.* **2003**, *28*, 222.
(52) Veryazov, V.; Widmark, P.-O.; Serrano-Andres, L.; Lindh, R.; Roos, B. O. *Int. J. Quantum Chem.* **2004**, *100*, 626.
(53) Ahlrichs, R.; Bär, M.; Häser, M.; Horn, H.; Kölmel, C. *Chem. Phys. Lett.* **1989**, *162*, 165. In the calculations, version 5.7 was used, see http://www.cosmologic.de.
(54) Richardson, W. H.; Peng, C.; Bashford, D.; Noodleman, L.; Case, D. A. *Int. J. Quantum Chem.* **1997**, *61*, 207.
(55) Schüürmann, G.; Cossi, M.; Barone, V.; Tomasi, J. *J. Phys. Chem. A* **1998**, *102*, 6706.
(56) Liptak, M. D.; Gross, K. C.; Seybold, P. G.; Feldgus, S.; Shields, G. C. *J. Am. Chem. Soc.* **2002**, *124*, 6421.
(57) Pliego, J. R., Jr.; Riveros, J. M. *J. Phys. Chem. A* **2002**, *106*, 7434.
(58) Almerindo, G. I.; Tondo, D. W.; Pliego, J. R., Jr. *J. Phys. Chem. A* **2004**, *108*, 166.
(59) Magill, A. M.; Yates, B. F. *Aust. J. Chem.* **2004**, *57*, 1205.
(60) Klicić, J. J.; Friesner, R. A.; Liu, S.-Y.; Guida, W. C. *J. Phys. Chem. A* **2002**, *106*, 1327.
(61) Mujika, J. I.; Mercero, J. M.; Lopez, X. *J. Phys. Chem. A* **2003**, *107*, 6099.
(62) Saracino, G. A. A.; Improta, R.; Barone, V. *Chem. Phys. Lett.* **2003**, *373*, 411.
(63) Fu, Y.; Liu, L.; Li, R.-Q.; Liu, R.; Guo, Q.-X. *J. Am. Chem. Soc.* **2004**, *126*, 814.
(64) Takano, Y.; Houk, K. N. *J. Chem. Theory Comput.* **2005**, *1*, 70.
(65) Jang, Y. H.; Sowers, L. C.; Çağin, T.; Goddard, W. A., III. *J. Phys. Chem. A* **2001**, *105*, 274.
(66) Jang, Y. H.; Goddard, W. A., III; Noyes, K. T.; Sowers, L. C.; Hwang, S.; Chung, D. S. *J. Phys. Chem. B* **2003**, *107*, 344.
(67) Cross, J. B.; Duca, J. S.; Kaminski, J. J.; Madison, V. S. *J. Am. Chem. Soc.* **2002**, *124*, 11004.
(68) Quenneville, J.; Popović, D. M.; Stuchebrukhov, A. A. *J. Phys. Chem. B* **2004**, *108*, 18383.
(69) Klingen, A. R.; Ullmann, G. M. *Biochemistry* **2004**, *43*, 12383.
(70) This approximation can be inferred from the possibility to exactly express (using similar notation) the total adiabatic gas-phase electronic energy of S_1 as $E_{gas}^{S_1} = E_{gas}^{S_0}|_{\mathbf{R}=\mathbf{R}(S_1)} + \omega_{gas}^{(S_1-S_0)}|_{\mathbf{R}=\mathbf{R}(S_1)}$.
(71) Heyne, K.; Herbst, J.; Stehlik, D.; Esteban, B.; Lamparter, T.; Hughes, J.; Diller, R. *Biophys. J.* **2002**, *82*, 1004.
(72) Sineshchekov, V. A. *Biochim. Biophys. Acta* **1995**, *1228*, 125.
(73) Foresman, J. B.; Head-Gordon, M.; Pople, J. A.; Frisch, M. J. *J. Phys. Chem.* **1992**, *96*, 135.
(74) Nielsen, I. B.; Åxman, Petersen, M.; Lammich, L.; Brøndsted Nielsen, M.; Andersen, L. H. *J. Phys. Chem. A* **2006**, *110*, 12592.
(75) Förster, T. *Z. Elektrochem. Angew. Phys. Chem.* **1950**, *54*, 531.
(76) Weller, A. *Prog. React. Kinet.* **1961**, *1*, 189.
(77) Shizuka, H. *Acc. Chem. Res.* **1985**, *18*, 141.
(78) Wan, P.; Shukla, D. *Chem. Rev.* **1993**, *93*, 571.
(79) Tolbert, L. M.; Solntsev, K. M. *Acc. Chem. Res.* **2002**, *35*, 19.
(80) Agmon, N. *J. Phys. Chem. A* **2005**, *109*, 13.
(81) One pK_a unit corresponds to a free-energy difference of about 0.06 eV at $T = 298.15$ K.